Nanoscale

PAPER

View Article Online
View Journal | View Issue

Check for updates

Cite this: *Nanoscale*, 2019, **11**, 15871

Single molecule *vs.* large area design of molecular electronic devices incorporating an efficient 2-aminepyridine double anchoring group†‡

L. Herrer,§[a,b] A. Ismael,§[c,d] S. Martín,[a,e] D. C. Milan,[f] J. L. Serrano,[b,e,g]* R. J. Nichols,[e]* C. Lambert[c]* and P. Cea[a,b,f]*

When a molecule is bound to external electrodes by terminal anchor groups, the latter are of paramount importance in determining the electrical conductance of the resulting molecular junction. Here we explore the electrical properties of a molecule with bidentate anchor groups, namely 4,4′-(1,4-phenylenebis(ethyne-2,1-diyl))bis(pyridin-2-amine), in both large area devices and at the single molecule level. We find an electrical conductance of 0.6×10^{-4} G_0 and 1.2×10^{-4} G_0 for the monolayer and for the single molecule, respectively. These values are approximately one order of magnitude higher than those reported for monodentate materials having the same molecular skeleton. A combination of theory and experiments is employed to understand the conductance of monolayer and single molecule electrical junctions featuring this new multidentate anchor group. Our results demonstrate that the molecule has a tilt angle of 30° with respect to the normal to the surface in the monolayer, while the break-off length in the single molecule junction occurs for molecules having a tilt angle estimated as 40°, which would account for the difference in their conductance values per molecule. The bidentate 2-aminepyridine anchor is of general interest as a contact group, since this terminal functionalized aromatic ring favours binding of the adsorbate to the metal contact resulting in enhanced conductance values.

Received 4th July 2019,
Accepted 6th August 2019

DOI: 10.1039/c9nr05662a

rsc.li/nanoscale

Open Access Article. Published on 07 August 2019. Downloaded on 3/28/2024 8:15:32 PM.
This article is licensed under a Creative Commons Attribution 3.0 Unported Licence.

Introduction

Research activity in molecular electronics has seen much development and growth in recent years as reflected in some recent reviews.[1–12] The aim of molecular electronics is to study individual molecules and their ensembles to understand their intrinsic electrical properties and, eventually, to use these functional materials as basic elements in circuitry at the nanoscale. As a result of these investigations, the first molecular electronic device for audio processing has already reached the market.[13] At a fundamental level, recent advances have identified the challenges to be overcome before a full implementation of this technology is achieved (most probably in combination with traditional silicon based current technologies). Among these challenges, the anchor group is of paramount importance for the formation of robust molecular junctions that result in high values of molecular conductance.[1] In this context, a comprehensive study of different anchor groups has been systematically performed by several research groups. These studies include monodentate molecules using anchor groups such as thiols[14–17] amines,[14,18,19] methyl sulfides,[20] selenols,[21,22] cyano,[23,24] isocyanides,[25] nitriles,[26] hydroxyl,[27] ethynylbenzenes,[28] isothiocyanates,[29] pyridines,[30–34] N-heterocyclic carbenes,[35] dimethylphosphine,[36] dihydrobenzo[*b*]thiophenes,[37] 4-(methylthio)phenyl groups,[38] thienyl rings,[39] diphenylphosphines,[40] trimethylsilylethynyl,[41–43] tetrathiofulvalenes,[44] triazatriangulenes,[45] and fullerenes.[46–48] More recently, bidentate molecules such as carboxylic acids,[47,49,50] carbodithioates,[51,52] dithiocarbamates,[53,54] norbornyldithiol,[55] cathecols,[56] or pyrazole[57] and also multipodal platforms[58–63]

[a]*Departamento de Química Física, Facultad de Ciencias, Universidad de Zaragoza, 50009 Zaragoza, Spain. E-mail: pilarcea@unizar.es*
[b]*Instituto de Nanociencia de Aragón (INA) and Laboratorio de Microscopias Avanzadas (LMA), Edificio I+D Campus Río Ebro, Universidad de Zaragoza, C/Mariano Esquillor, s/n, 50018 Zaragoza, Spain. E-mail: joseluis@unizar.es*
[c]*Department of Physics, University of Lancaster, Lancaster, LA1 4YB, UK. E-mail: c.lambert@lancaster.ac.uk*
[d]*Department of Physics, College of Education for Pure Science, Tikrit University, Tikrit, Iraq*
[e]*Department of Chemistry, University of Liverpool, Crown Street, Liverpool, L69 7ZD, UK. E-mail: R.J.Nichols@liverpool.ac.uk*
[f]*Instituto de Ciencia de Materiales de Aragón (ICMA), Universidad de Zaragoza-CSIC, 50009 Zaragoza, Spain*
[g]*Departamento de Química Orgánica, Facultad de Ciencias, Universidad de Zaragoza, 50009 Zaragoza, Spain*

†Raw I(s), *I–V* spectroscopy are available at the Data Catalogue DOI: 10.17638/datacat.liverpool.ac.uk/906

‡Electronic supplementary information (ESI) available: Further discussion of the synthetic details, experimental procedures and DFT calculations. See DOI: 10.1039/c9nr05662a

§These authors contributed equally to this work.

Open Access Article. Published on 07 August 2019. Downloaded on 3/28/2024 8:15:32 PM.
This article is licensed under a Creative Commons Attribution 3.0 Unported Licence.

have been explored, with a view to improving the conductance and stability of the devices.

A key contemporary focus in the field of molecular electronics is electrical properties of individual molecules, although in view of potential future applications and construction of device-like structures more compatible with conventional fabrication strategies, the assembly of molecules in large area devices continued to develop and grow in interest.[2] These large area devices can be fabricated by bottom-up technologies such as self-assembly (SA) and Langmuir–Blodgett (LB) methods. In SA, chemisorption of the organic material onto the metal electrode occurs first and subsequent molecular organization is driven by supra-molecular interactions from the packing such as van der Waals, force π–π overlap interactions and hydrophobic forces. In LB films, the molecules are first ordered at the air–water interface and later they are physi- or chemisorbed onto a solid substrate, upon the transference of the Langmuir films onto the substrate.[64] The LB method results, after appropriate optimization of certain parameters, in tightly-packed and homogeneous monolayers, which is a critical issue in the mass production of devices with a reproducible behaviour. Moreover, the production costs are relatively low, since a Langmuir trough is operated in ambient conditions and from a technical viewpoint the procedure is relatively straightforward. Additionally, these LB monolayers can be deposited onto virtually any substrate, which is particularly important given the determining role that the electrode–molecule interface plays in molecular junctions. Thus, the use of directionally aligned molecular films prepared using LB methods has provided a template for investigating a diverse variety of organic–metal contacts.[34,44,49,65–69]

In this contribution we study the electrical properties of an oligophenyleneethynylene (OPE) derivative, 4,4′-(1,4-phenylenebis(ethyne-2,1-diyl))bis(pyridin-2-amine), compound **1**. Compound **1** is a symmetrical, bidentate molecule with a highly conjugated structure. This new compound is studied here as a single molecule and when assembled in a Langmuir–Blodgett monolayer. Similar studies with other types of OPEs have typically shown identical conductance values for compounds acting as individual molecule or as a LB or SA monolayer.[2,32,49,66,70] Charge transport across such short OPE molecular junctions takes place by tunneling and therefore *I–V* traces might be expected to exhibit similar shapes and conductance values regardless of aggregation effects or interactions between neighbouring molecules in the film.[2] However, compound **1** displays certain differences in the conductance per molecule of a single molecule and when assembled in a monolayer. Additionally, we find that compound **1** has higher conductance values than those reported for the same OPE backbone, but with monodentate anchoring groups. Informed by theoretical calculations, we interpret these results in terms of a different preferential orientation of the molecules in the monolayer and in the single molecule junction, as well as in terms of the chemisorption of the bidentate anchor group onto the bottom and possibly the top-contact electrode.

Experimental

Synthesis of 1

Tert-butyl (4-iodopyridin-2-yl)carbamate (0.67 g, 2.1 mmol), 1,4-diethynylbenzene (0.124 g, 0.985 mmol), $Pd(PPh_3)_4$ (10% mol), CuI (10% mol) and dry triethylamine (12 mL) were stirred under inert conditions at 60 °C for 20 h in a Schlenk flask. The solvent was removed and the crude product thoroughly washed with Milli-Q water, aqueous saturated brine solution, THF, NH_4OH (aq.), diethyl ether and hexane by a milling process. This intermediate, di-*tert*-butyl (4,4′-(1,4-phenylenebis(ethyne-2,1-diyl))bis(pyridine-4,2-diyl))dicarbamate, named compound *A*, was obtained as an off-white powder with a yield of 83%. Compound *A* (0.421 g, 0.82 mmol), was dissolved in trifluoroacetic acid (5 mL) and stirred 1 h at room temperature. Milli-Q water (20 mL) was added to the reaction flask and the solution was neutralized with aqueous sodium bicarbonate. The mixture was extracted with ethyl acetate and the organic phase washed with water, saturated aqueous brine solution, and evaporated to dryness to afford the product. The obtained whitish powder was triturated in a filter plate with Milli-Q water and hexane to afford 0.174 g of pure compound **1**, Fig. 1. Yield: 69%. ^{1}H NMR (500 MHz, DMSO-d_6, δ (ppm)): 7.94 (d, 2H), 7.62 (s, 4H), 6.60 (d, 2H), 6.56 (s, 2H), 6.12 (s, 4H). ^{13}C NMR (125 MHz, DMSO-d_6, δ (ppm)): 159.89, 148.41, 131.97, 130.24, 122.28, 113.26, 109.41, 90.59, 89.82. EM (*m*/*z*): 311.4 (M + 1). Further details, including the NMR spectra, are available in the ESI.‡

NMR spectra were performed on Bruker advanced spectrometers at 400/500 MHz for ^{1}H NMR and 100/125 MHz for ^{13}C NMR. MALDI-TOF mass spectra was performed on an Autoflex mass spectrometer from Bruker using dithranol as matrix.

Fabrication of the LB monolayers

Langmuir films were fabricated by spreading 2.3 mL of a 2.5×10^{-5} M solution of compound **1** in a solvent mixture of DMSO : $CHCl_3$ (1 : 4). The trough used to prepare the Langmuir films was a NIMA 702 BAM (700 × 100 mm^2). A lateral mechanical compression of the film was applied with the aid of a mobile barrier swept at a speed of 12 cm^2 min^{-1}. Under these experimental conditions reproducible surface pressure *vs.* area per molecule (*π*–*A*) isotherms recorded at 20 °C were obtained (Fig. S4c‡). Langmuir films were transferred when a target area of 0.26 nm^2 per molecule (π = 8 mN m^{-1}) was achieved. The substrate was withdrawn from the water subphase at 2 mm min^{-1}.

AFM images were obtained through deployment of a Multimode 8 microscope in combination with a Nanoscope V control unit from Bruker operating under ambient air con-

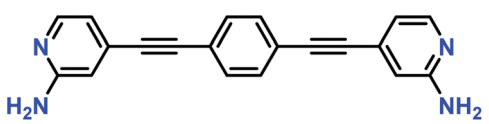


Fig. 1 Molecular structure of compound **1**, 4,4′-(1,4-phenylenebis(ethyne-2,1-diyl))bis(pyridin-2-amine).

This journal is © The Royal Society of Chemistry 2019

Open Access Article. Published on 07 August 2019. Downloaded on 3/28/2024 8:15:32 PM.
This article is licensed under a Creative Commons Attribution 3.0 Unported Licence.

ditions. Images were recorded at a scan rate of 0.5–1.2 Hz, in tapping and Peak-Force modes. RTESPA-150 (150–210 kHz, 5–10 N m^{-1}, nominal radius of 8 nm) and ScanAsyst Air (70–95 kHz, 0.5–0.8 N m^{-1}, nominal radius of 2 nm) tips were employed. Image analysis was carried out off-line with the Nanoscope V1.40 software package.

A Kratos AXIS ultra DLD spectrometer with a monochromatic Al Kα X-ray source (1486.6 eV) using a pass energy of 20 eV was employed to register the X-ray photoelectron spectroscopy (XPS) spectra of the LB films of compound **1** or self-assembled (SA) films of 2-aminepyridine. The photoelectron take-off angle was 90° with respect to the sample plane. All the XPS binding energies were referenced to the C(1s) peak at 284.6 eV to provide a precise energy calibration.

$I(s)$ curves for determining the single molecule conductance and I–V curves for large area conductance characterization, were registered by using an Agilent 5500 STM controller assisted by the Agilent Picoscan 5.3.3 software. STM tips were prepared from commercially available Au wires (99.99%, 0.25 mm diameter, Goodfellow). Sample preparation for the single-molecule measurements using the $I(s)$ technique[1] was achieved using a clean and flame annealed gold substrate (Arrandee™) which was immersed for 1 min into a 1×10^{-4} M solution of compound **1** in dry dimethylformamide (DMF). DMF was previously degassed by three freeze–pump–thaw cycles. After this short-term incubation, the sample was copiously rinsed with methanol and distilled water followed by a drying process under a N_2 stream. Measurements were carried out in previously deoxygenated mesitylene. $I(s)$ curves were recorded from different samples equally prepared. Initial tip–substrate distance (s_0) was determined by an initial calibration with I_0 = 30 nA (set point current) and U_t = 0.3 V (tip bias) as set point parameters (Fig. S7‡). The TTC (touch-to-contact) method for the determination of the molecular conductance in a monolayer has been detailed before.[70] In this contribution, 21 $I(s)$ curves were recorded to calibrate the initial tip–substrate distance (s_0) with I_0 = 10 nA and U_t = 0.6 V as set point parameters, obtaining a value of $(d\ln(I)/ds) = 6.9 \pm 1.3$ nm^{-1} (details in the ESI, Fig. S8‡). Subsequently, I–V curves were registered in air conditions at 1.6 nm tip–substrate distance (s) using as set-point parameters I_0 = 0.9 nA and U_t = 0.6 V.

Theory

The density functional (DFT) code SIESTA[71] was used to obtain optimum geometries of the isomers located between gold electrodes (see ESI‡ for detailed structures). We used a double-zeta plus polarization orbital basis set, norm-conserving pseudopotentials, the local density approximation (LDA) exchange correlation functional, and to define the real space grid, an energy cutoff of 200 Rydbergs. Structures were relaxed until all forces on the atoms were less than 0.05 eV $Å^{-1}$. For conductance calculations, the LDA functional was employed. For binding energy calculations a van der Waals functional was used (for more details, see the binding energy sections of the ESI‡). The DFT mean field Hamiltonian was combined with the quantum transport code Gollum[72] to obtain the transmission coefficient $T(E)$ for electrons of energy E passing through the junction. Results were also computed using GGA and it was found that the resulting transmission functions were comparable[57,73] to those obtained using LDA. To simulate the likely contact configuration during a break-junction experiment,[74,75] a device with a flat bottom electrode constructed from 6 layers of Au (111), each containing 30 gold atoms, and a top electrode terminated by a pyramid of gold atoms was modeled.

Results and discussion

Electrical properties of compound **1** were studied both at the single-molecule level and in Langmuir–Blodgett (LB) monolayers. Fig. 2 shows the experimental results for their electrical properties. More than 200 I–V curves were recorded to determine the electrical properties of compound **1** in a LB monolayer. These curves were recorded from different samples and also at different locations on the same sample by the TTC method.[76] Using calibration procedures previously described the STM tip was located at 1.6 ± 0.1 nm from the gold surface. This separation coincides with the measured monolayer thickness determined by scratching the LB film sample with the AFM tip (see Fig. 2d and ESI section B.2‡). The length of the molecule estimated from the software Spartan®08 is 1.8 nm. Accordingly, compound **1** in the LB films has a tilt angle (θ) of *ca.* 30° with respect to the normal of the gold substrate. Fitting the low-voltage region (−0.5 to +0.5 V) where the I–V curve is almost linear (the ohmic region), a conductance value of 0.6×10^{-4} G_0 is obtained, Fig. 2a. Additionally, the single-molecule conductance for compound **1** was obtained from more than 250 single $I(s)$ traces recorded from different freshly prepared samples as shown in Fig. 2b. On the basis of the different binding energies of the contacting groups (amine *versus* pyridine) and their different positions in the molecule (the pyridyl nitrogen is set back from the amine one) one might expect to see multiple plateaus during the junction stretching and breaking. The pyridine–Au contact is reported to have a binding energy which depends on tilt angle (1.03 eV for a tilt angle of 50°),[77] while the amine to gold contact is weaker (binding energy of 0.6 eV)[78] and does not depend significantly on the orientation of the anchoring group. However, only single plateaus are generally resolved. This would imply that the junction breaking process is a concerted process, which may involve movement or deformation of gold atoms of the contact. A 1D histogram was built from all the current *versus* distance curves exhibiting a discernible maxima at 1.2×10^{-4} G_0, which is associated to the most probable value for the single molecule conductance Fig. 2c. This value is significantly higher than the conductance per molecule of **1** in an LB film. The break-off distance determined for compound **1**, is 1.35 ± 0.1 nm (Fig. 2f and ESI section E‡). Taking into account the length of the molecule, compound **1** exhibits a tilt angle of ~40° with respect to the normal of the gold substrate. Fig. 2e shows a comparison between the I–V curve for the monolayer (average of 250 curves) determined by the TTC method and the

Open Access Article. Published on 07 August 2019. Downloaded on 3/28/2024 8:15:32 PM.
This article is licensed under a Creative Commons Attribution 3.0 Unported Licence.

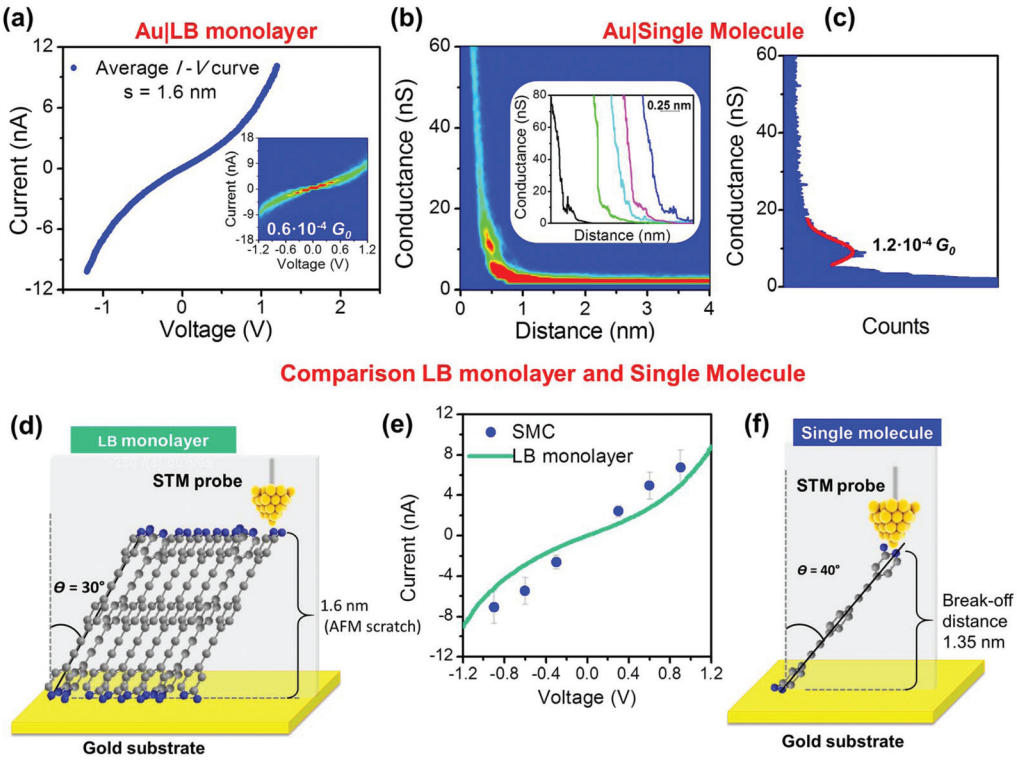


Fig. 2 (a) Average *I*–*V* curve recorded at a tip–substrate distance of 1.6 nm using the TTC method. Inset: 2D histogram containing all traces recorded. (b) 2D histogram recorded by the *I*(*s*) method containing all traces recorded. Inset: examples of *I*(*s*) single traces; the *x* axis has been displaced for clarity (U_t = 0.6 V and I_0 = 60 nA). (c) 1D histogram and Gauss peak fitting. (d) Scheme showing the inclination of the molecules in the LB monolayer, forming a tilt angle of 30° with respect to the normal to the surface. (e) *I*–*V* curves for the single molecule and the monolayer (f) scheme showing a single molecular junction with a break-off distance of 1.35 nm, *i.e.*, a tilt angle of the molecule of 40°.

single molecule data recorded by the *I*(*s*) method (determined as described in the ESI, section C‡).

Generally, the electrical conductance for single molecules and monolayers of the same compound in a tunnelling regime has been reported to be the same.[32,66,79] An exception here has been interpreted in terms of H-bonds between neighbouring molecules preventing a good interaction between the carboxylic terminal group and the gold STM tip[80] or some restriction of the molecule in a certain orientation.[34] Theoretical calculations were performed in order to understand why the electrical conductance per molecule of compound **1** as a single molecule, differs from that of an assembled LB monolayer and how the two potential anchor positions (pyridine-N and amine-N) of compound **1** (see Table S2 in the ESI‡) lead to an increase in conductance, compared with compounds having the same chemical structure, but a single anchor group.

DFT results indicate that a single molecule of compound **1** prefers to have a polar (tilt) angle in the range $\theta \approx 29$–$42°$ (Fig. S15‡) and an azimuthal angle $\phi = 0°$ (Fig. S16‡), which is consistent with the measured tip–substrate distance (Table S1‡). According to our calculations, in dimers of compound **1** (π-stacked), the distance between the two molecules is D = 3.0 Å and their displacement (due to mutual sliding) is X = 1.4 Å (for more details see Fig. S19 and S20‡). In contrast, the most energetically favorable tilt angle for compound **1** in the LB monolayer is found to be *ca.* 30°, which is lower than that obtained for the single molecule (see Fig. S26‡). These theoretical results are consistent with the tilt angle of 30° obtained from the experimental LB monolayer thickness and the experimental tilt angle of 40°, as determined from the experimental break-off distance. In these configurations, the molecule-gold substrate junction is formed through chemisorption of both the pyridine and the amine nitrogen. To test out the tendency of this anchor group to chemisorb on gold (Fig. 3a) through both the pyridine-N and the amine-N, the XPS spectrum of a chosen reference compound, namely the 2-aminepyridine, was recorded. The XPS powder spectrum of 2-aminepyridine exhibits a signal unveiling two peaks: one at 398.7 eV, attributed to the pyridine-N, and another one at 399.8 eV assigned to the amine-N.[81] The deconvolution of the XPS spectrum of a self-assembled monolayer (SAM) of 2-aminepyridine also results in two peaks that show a binding energy displacement of 0.7 eV for both the pyridine-N and the amine-N with respect to their corresponding peaks in the powder spectrum. This result is indicative of chemisorption of 2-aminepyridine onto the gold surface through both the pyridine and the amine groups. The XPS powder spectrum registered for compound **1** can also be deconvoluted into two peaks at 398.4 and 398.9 eV attributable to the pyridine-N and the amine-N, respectively. The deconvolution of the XPS spectrum of the LB monolayer of compound

 This journal is © The Royal Society of Chemistry 2019

Open Access Article. Published on 07 August 2019. Downloaded on 3/28/2024 8:15:32 PM.
This article is licensed under a Creative Commons Attribution 3.0 Unported Licence.

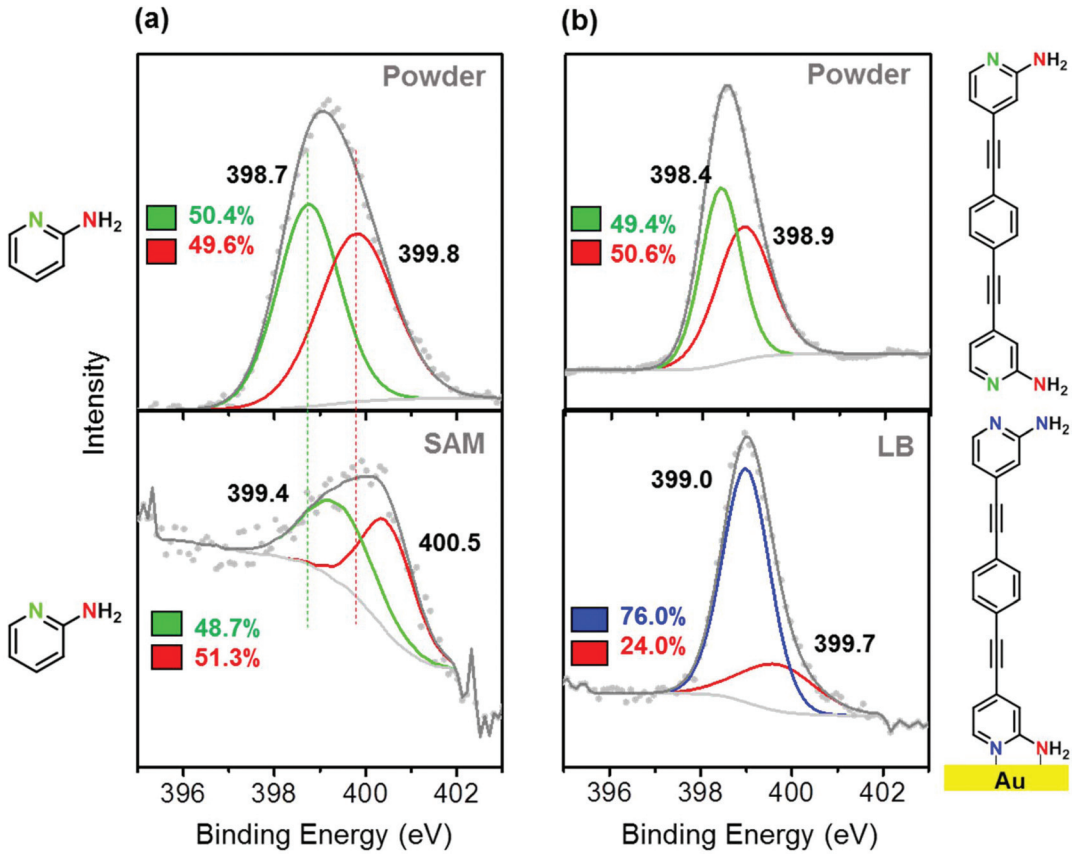


Fig. 3 (a) Powder and SAM XPS spectra of the reference compound 2-aminepyridine. (b) Powder and LB monolayer XPS spectra of compound **1**.

1 results in an intense peak at 399.0 eV and a weaker one at 399.7 with *ca.* a 3 : 1 ratio. This may indicate that the peak at 399.0 eV corresponds to three of the four nitrogen atoms contained in the molecule. We interpret the broad peak at 399.0 eV as the combined contribution of the chemisorbed pyridine-N (*ca.* at 399.4 eV as directly taken from the 2-aminepyridine chemisorbed material) along with free pyridine-N (398.4 eV as in the powder of **1**) and the free amine-N (at 398.9 eV as in the powder of **1**). Additionally, the band at 399.7 eV is attributable to the chemisorbed amine-N, in good agreement with the shift observed for the chemisorbed amine-N in the reference compound.

Fig. S27‡ shows that a pyramidal electrode tip optimally bound to one gold atom *via* a Au–N (pyridine) bond, rather than being positioned between molecules or on top of the amine group ($-NH_2$). After optimization of the key parameters including: distance d, tilt angle θ, azimuthal angle ϕ, separation distance D and displacement distance X, the transmission coefficients were calculated for both the single molecule and the monolayer. DFT calculations indicate that the transmission coefficient is slightly higher for the single molecule than for the monolayer (Fig. 4, red and black dotted lines in the left panel). Fig. S30‡ demonstrates that the transmission coefficient of a monolayer with n-molecules converge rapidly with increasing n and in fact is very close to that of a dimer (n = 2). Therefore, calculations of transport through a dimer are sufficient to model the properties of a monolayer and for simplicity it will be utilized henceforth. In these calculations, the tilt angle, θ, for both the single molecule and for the molecules in the monolayer has been chosen to correspond to the measured break-off distance and to the monolayer thickness, respectively. The red-dashed vertical rectangle in the left panel of Fig. 4 shows that over a wide range of energy within the HOMO–LUMO gap, there is an excellent agreement between measured and calculated conductance values both qualitatively and quantitatively.

Dotted lines in Fig. 4 correspond to a simulation based on a flat substrate and pyramidal tip. Since the shape of the top contact in our experiments is not known, we also simulated a junction with both top and bottom flat electrodes. Solid lines in Fig. 4 show that the conductance of a flat–flat junction is higher than that of a flat–tip junction. This result indicates that a flat electrode may favor a double anchoring of the molecule resulting in a higher conductance. Importantly, the ratio of conductances between monomer and monolayer remains approximately unchanged when flat–tip and flat–flat configurations are compared with each other. Table 1 summarizes these results.

For both the single molecule and the monolayer, the conductance values of compound **1** are significantly higher (nearly one order of magnitude) than those previously reported for

Open Access Article. Published on 07 August 2019. Downloaded on 3/28/2024 8:15:32 PM.
This article is licensed under a Creative Commons Attribution 3.0 Unported Licence.

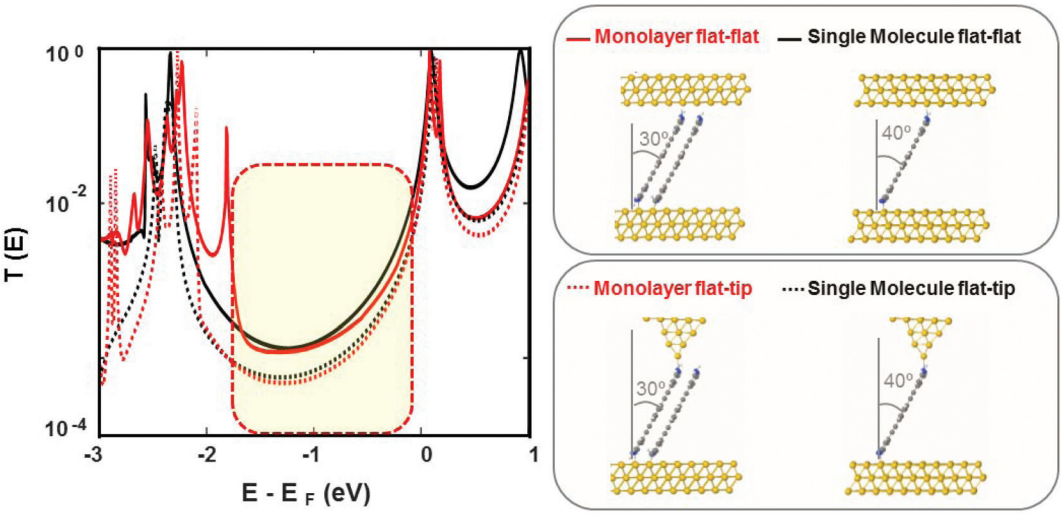
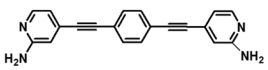
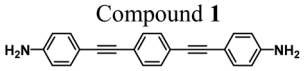
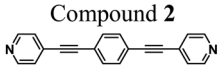


Fig. 4 Left panel: Zero bias transmission coefficients as a function of the electron energy E, for the single molecule (black curve) and the monolayer (red curve). Dotted lines correspond to the flat–tip electrode configuration and solid line to the flat–flat configuration. Right panel: Cartoons illustrating the four gold junctions corresponding to the transmission coefficients shown in the left panel.

Table 1 Experimental and theoretical conductance values ($E - E_F = -0.5$ eV)

	Experimental conductance value (G_0)	Tilt angle from experimental data (θ)	Theoretical conductance value (G_0)	Theoretical conductance value (G_0)
			Flat–tip configuration	Flat–flat configuration
Single molecule	1.2×10^{-4}	~40°	2.3×10^{-4}	5.7×10^{-4}
LB monolayer	0.6×10^{-4}	~30°	1.8×10^{-4}	4.0×10^{-4}

Table 2 Conductance for OPE derivatives with amine and pyridine terminal groups as well as with a double anchoring group incorporating amine and pyridine as single molecules (I(s) method) or in monolayers (either Langmuir–Blodgett of self assembled films, TTC method)

Molecule	Single molecule (G_0)	Monolayer (G_0)
	1.2×10^{-4}	0.6×10^{-4}
	This contribution	This contribution
Compound **1**		
	2.4×10^{-5}	—
	Ref. 19	
Compound **2**		
	5.4×10^{-5}	5.2×10^{-5}
	Ref. 32	Ref. 32
Compound **3**		

compounds with a similar chemical structure (see Table 2 and Table S2‡). Remarkably, while compound **2**, *i.e.* an amine terminal OPE derivative shows a conductance of 2.4×10^{-5} G_0 and compound **3**, *i.e.* a pyridine terminal OPE, has a conductance of 5.4×10^{-5} G_0, compound **1** exhibits a conductance value for the single molecule of 1.2×10^{-4} G_0. These results, together with those reported for other multidentated anchor groups (Table S2‡) are indicative of improved, robust, and stable molecular junctions favored through the double anchoring that promotes an efficient electrical transport in the molecular junction.

Conclusions

There are relatively few studies in the literature reporting molecular junctions of bidentate anchor groups, but the results published so far suggest that such groups may result in molecular junctions with improved conductance and stability. Our exploration of a double anchor group, formed from 2-amine-pyridine reveals a conductance value one order of magnitude larger than *state-of-the-art* monodentate materials of OPE derivatives with the same molecular structure. High quality LB films also show larger conductance values than those reported for other OPEs. Additionally, the experimental results indicate that compound **1** exhibits a larger conductance in the single molecule state than in the LB films. Calculated transmission coefficients, $T(E)$, confirm the experimental results showing a lower conductance value for the monolayer compared to the single molecule. This lower conductance arises from different orientations of the single molecule compared with those in the LB monolayer, as demonstrated by AFM, XPS, STM, and

 This journal is © The Royal Society of Chemistry 2019

theoretical calculations. The improved conductance of compound **1**, favored by a chemisorption of the molecule by both the amine and the pyridine nitrogen atoms onto the bottom electrode, generates new expectations for the development of improved molecular junctions by the use of bidentate anchoring groups.

Conflicts of interest

There are no conflicts to declare.

Acknowledgements

P. C. and J. L. S. are grateful for financial assistance from Ministerio de Economía y Competitividad from Spain and fondos FEDER in the framework of projects MAT2016-78257-R, CTQ2015-70174-P and PGC2018-097583-B-I00. J. L. S. also acknowledges the funded project Hierarchical Self Assembly of Polymeric Soft Systems, "SASSYPOL", from the 7th Framework Programme (CEE, Ref-607602). L. H., S. M., J. L. S, and P. C. acknowledge support from DGA/Fondos FEDER (construyendo Europa desde Aragón) for funding PLATON (E31_17R) and CLIP (E47_17R) research groups. R. J. N. thanks EPSRC for funding (EP/M029522/1, EP/M005046/1 and EP/K007785/1). A. K. I. and C. J. L. acknowledge financial support from the UK EPSRC, through grant no. EP/M014452/1, EP/P027156/1 and EP/N03337X/1. This work was additionally supported by the European Commission is provided by the FET Open project 767187 – QuIET and the EU project Bac-to-Fuel. A. K. I. is grateful for financial assistance from Tikrit University (Iraq), and the Iraqi Ministry of Higher Education (SL-20). The authors also thank Dr Andrea Vezzoli for useful discussions.

Open Access Article. Published on 07 August 2019. Downloaded on 3/28/2024 8:15:32 PM.
This article is licensed under a Creative Commons Attribution 3.0 Unported Licence.

References

1 N. Xin, J. Guan, C. Zhou, X. Chen, C. Gu, Y. Li, M. A. Ratner, A. Nitzan, J. F. Stoddart and X. Guo, Concepts in the design and engineering of single-molecule electronic devices, *Nat. Rev. Phys.*, 2019, **1**, 211–230.

2 A. Vilan, D. Aswal and D. Cahen, Large-Area, Ensemble Molecular Electronics: Motivation and Challenges, *Chem. Rev.*, 2017, **117**, 4288–4286.

3 A. Vilan and D. Cahen, Chemical Modification of Semiconductor Surfaces for Molecular Electronics, *Chem. Rev.*, 2017, **117**, 4624–4666.

4 D. Xiang, X. Wang, C. Jia, T. Lee and X. Guo, Molecular-scale electronics: from concept to function, *Chem. Rev.*, 2016, **7**, 4318–4440.

5 T. A. Su, M. Neupane, M. L. Steigerwald, L. Venkataraman and C. Nuckolls, Chemical principles of single-molecule electronics, *Nat. Rev. Mater.*, 2016, **1**, 16002.

6 Y. Komoto, S. Fujii, M. Iwane and M. Kiguchi, Single-molecule junctions for molecular electronics, *J. Mater. Chem. C*, 2016, **4**, 8842–8858.

7 E. Leary, A. La Rosa, M. T. Gonzalez, G. Rubio-Bollinger, N. Agrait and N. Martín, Incorporating single molecules into electrical circuits. The role of the chemical anchoring group, *Chem. Soc. Rev.*, 2015, **44**, 920.

8 R. M. Metzger, Unimolecular Electronics, *Chem. Rev.*, 2015, **115**, 5056–5115.

9 R. J. Nichols and S. J. Higgins, Single-Molecule Electronics: Chemical and Analytical Perspectives, *Annu. Rev. Anal. Chem.*, 2015, **8**, 389–417.

10 L. Sun, Y. A. Diaz-Fernández, T. A. Gschneidtner, F. Westerlund, S. Lara-Avila and K. Moth-Poulsen, Single-molecule electronics: from chemical design to functional devices, *Chem. Soc. Rev.*, 2014, **43**, 7378–7411.

11 C. Jia and X. Guo, Molecule-electrode interfaces in molecular electronic devices, *Chem. Soc. Rev.*, 2013, **42**, 5642–5660.

12 A. Aaaaa, Editorial Visions for a molecular future, *Nat. Nanotechnol.*, 2013, **8**, 385–389.

13 A. J. Bergren, L. Zeer-Wanklyn, M. Semple, N. Pekas, B. Szeto and R. L. McCreery, Musical molecules: the molecular junction as an active component in audio distortion circuits, *J. Phys.: Condens. Matter*, 2016, **28**, 094011.

14 F. Chen, X. Li, J. Hihath, Z. Huang and N. Tao, Effect of Anchoring Groups on Single-Molecule Conductance: Comparative Study of Thiol-, Amine-, and Carboxylic-Acid-Terminated Molecules, *J. Am. Chem. Soc.*, 2006, **128**, 15874–15881.

15 D. Dulic, F. Pump, S. Campidelli, P. Lavie, G. Cuniberti and A. Filoramo, Controlled Stability of Molecular Junctions, *Angew. Chem., Int. Ed.*, 2009, **48**, 8273–8276.

16 I. Diez-Perez, Z. Li, J. Hihath, J. Li, C. Zhang, X. Yang, L. Zang, Y. Dai, X. Feng, K. Muellen and N. Tao, Gate-controlled electron transport in coronenes as a bottom-up approach towards graphene transistors, *Nat. Commun.*, 2010, **1**, 31.

17 E. Leary, A. La Rosa, M. T. González, G. Rubio-Bollinger, N. Agraït and N. Martín, Incorporating single molecules into electrical circuits. The role of the chemical anchoring group, *Chem. Soc. Rev.*, 2015, **44**, 920–942.

18 D. Venkataraman, J. E. Klare, C. Nuckolls, M. S. Hybertsen and M. L. Steigerwald, Dependence of single-molecule junction conductance on molecular conformation, *Nature*, 2006, **442**, 904–907.

19 R. R. Ferradás, S. Marqués-González, H. M. Osorio, J. Ferrer, P. Cea, D. C. Milan, A. Vezzoli, S. J. Higgins, R. J. Nichols, P. J. Low, V. M. García-Suárez and S. Santiago Martín, Low variability of single-molecule conductance assisted by bulky metal-molecule contacts, *RSC Adv.*, 2016, **6**, 75111–75121.

20 Y. S. Park, A. C. Whalley, M. Kamenetska, M. L. Steigerwald, M. S. Hybertsen, C. Nuckolls and L. Venkataraman, Contact Chemistry and Single-Molecule Conductance: A Comparison of Phosphines, Methyl Sulfides, and Amines, *J. Am. Chem. Soc.*, 2007, **129**, 15768–15769.

21 E. Adaligil, Y.-S. Shon and K. Slowinski, Effect of Headgroup on Electrical Conductivity of Self-Assembled

Open Access Article. Published on 07 August 2019. Downloaded on 3/28/2024 8:15:32 PM.
This article is licensed under a Creative Commons Attribution 3.0 Unported Licence.

Monolayers on Mercury: n-Alkanethiols versus n-Alkaneselenols, *Langmuir*, 2010, **26**, 1570–1573.

22 J. D. Monnell, J. J. Stapleton, S. M. Dirk, A. Reinerth, J. M. Tour, D. L. Allara and P. S. Weiss, Relative conductances of alkaneselenolate and alkanethiolate monolayers on Au{111}, *J. Phys. Chem. B*, 2005, **109**, 20343–20349.

23 A. Mishchenko, L. A. Zotti, D. Vonlanthen, M. Bürkle, F. Pauly, J. C. Cuevas, M. Mayor and T. Wandlowski, Single-Molecule Junctions Based on Nitrile-Terminated Biphenyls: A Promising New Anchoring Group, *J. Am. Chem. Soc.*, 2011, **133**, 184–187.

24 L. A. Zotti, T. Kirchner, J. C. Cuevas, F. Pauly, T. Huhn, E. Scheer and A. Erbe, Revealing the role of anchoring groups in the electrical conduction through single-molecule junctions, *Small*, 2010, **6**, 1529.

25 B. Kim, J. M. Beebe, Y. Jun, X. Y. Zhu and C. D. Frisbie, Correlation between HOMO alignment and contact resistance in molecular junctions: Aromatic thiols versus aromatic isocyanides, *J. Am. Chem. Soc.*, 2006, **128**, 4970–4971.

26 A. Beeby, K. Findlay, P. J. Low and T. B. Marder, A Re-evaluation of the Photophysical Properties of 1,4-Bis(phenylethynyl)benzene: A Model for Poly(phenyleneethynylene), *J. Am. Chem. Soc.*, 2002, **124**, 8280–8284.

27 Z. Li, M. Smeu, M. A. Ratner and E. Borguet, Effect of Anchoring Groups on Single Molecule Charge Transport through Porphyrins, *J. Phys. Chem. C*, 2013, **117**, 14890–14898.

28 L. Herrer, A. González-Orive, S. Marqués-González, S. Martín, R. J. Nichols, J. L. Serrano, P. J. Low and P. Cea, Electrically transmissive alkyne-anchored monolayers on gold, *Nanoscale*, 2019, **11**, 7976–7985.

29 C.-H. Ko, M.-J. Huang, M.-D. Fu and C.-H. Chen, Superior Contact for Single-Molecule Conductance: Electronic Coupling of Thiolate and Isothiocyanate on Pt, Pd, and Au, *J. Am. Chem. Soc.*, 2010, **132**, 756–764.

30 M. Kamenetska, S. Y. Quek, A. C. Whalley, M. L. Steigerwald, H. J. Choi, S. G. Louie, C. Nuckolls, M. S. Hybertsen, J. B. Neaton and L. Venkataraman, Conductance and Geometry of Pyridine-Linked Single-Molecule Junctions, *J. Am. Chem. Soc.*, 2010, **132**, 6817–6821.

31 W. Hong, D. Z. Manrique, P. Moreno-García, M. Gulcur, A. Mishchenko, C. J. Lambert, M. R. Bryce and T. Wandlowski, Single Molecular Conductance of Tolanes: Experimental and Theoretical Study on the Junction Evolution Dependent on the Anchoring Group, *J. Am. Chem. Soc.*, 2012, **134**, 2292–2304.

32 H. M. Osorio, S. Martin, M. Carmen Lopez, S. Marques-Gonzalez, S. J. Higgins, R. J. Nichols, P. J. Low and P. Cea, Electrical characterization of single molecule and Langmuir-Blodgett monomolecular films of a pyridine-terminated oligo(phenylene-ethynylene) derivative, *Beilstein J. Nanotechnol.*, 2015, **6**, 1145–1157.

33 B. Xu and N. J. Tao, Measurement of Single-Molecule Resistance by Repeated Formation of Molecular Junctions, *Science*, 2003, **301**, 1221.

34 H. M. Osorio, S. Martín, D. C. Milan, A. González-Orive, J. B. G. Gluyas, S. J. Higgins, P. J. Low, R. J. Nichols and P. Cea, Influence of surface coverage on the formation of 4,4′-bipyridinium (viologen) single molecular junctions, *J. Mater. Chem. C*, 2017, **5**, 11717–11723.

35 C. M. Crudden, J. H. Horton, I. I. Ebralidze, O. V. Zenkina, A. B. McLean, B. Drevniok, Z. She, H.-B. Kraatz, N. J. Mosey, T. Seki, E. C. Keske, J. D. Leake, A. Rousina-Webb and G. Wu, Ultra stable self-assembled monolayers of N-heterocyclic carbenes on gold, *Nat. Chem.*, 2014, **6**, 409.

36 Y. S. Park, A. C. Whalley, M. Kamenetska, M. L. Steigerwald, M. S. Hybertsen, C. Nuckolls and L. Venkataraman, Contact chemistry and single-molecule conductance: A comparison of phosphines, methyl sulfides, and amines, *J. Am. Chem. Soc.*, 2007, **129**, 15768–15769.

37 P. Moreno-Garcia, M. Gulcur, D. Z. Manrique, T. Pope, W. Hong, V. Kaliginedi, C. Huang, A. S. Batsanov, M. R. Bryce, C. J. Lambert and T. Wandlowski, Single-Molecule Conductance of Functionalized Oligoynes: Length Dependence and Junction Evolution, *J. Am. Chem. Soc.*, 2013, **135**, 12228–12240.

38 R. S. Klausen, J. R. Widawsky, M. L. Steigerwald, L. Venkataraman and C. Nuckolls, Conductive Molecular Silicon, *J. Am. Chem. Soc.*, 2012, **134**, 4541–4544.

39 C. R. Arroyo, E. Leary, A. Castellanos-Gómez, G. Rubio-Bollinger, M. T. González and N. Agraït, Influence of Binding Groups on Molecular Junction Formation, *J. Am. Chem. Soc.*, 2011, **133**, 14313–14319.

40 R. Parameswaran, J. R. Widawsky, H. Vázquez, Y. S. Park, B. M. Boardman, C. Nuckolls, M. L. Steigerwald, M. S. Hybertsen and L. Venkataraman, Reliable Formation of Single Molecule Junctions with Air-Stable Diphenylphosphine Linkers, *J. Phys. Chem. Lett.*, 2010, **1**, 2114–2119.

41 N. Katsonis, A. Marchenko, D. Fichou and N. Barret, Investigation on the nature of the chemical link between acetylenic organosilane self-assembled monolayers and Au (111) by means of synchrotron radiation photoelectron spectroscopy and scanning tunneling microscopy, *Surf. Sci.*, 2008, **602**, 9–16.

42 N. Katsonis, A. Marchenko, S. Taillemite, D. Fichou, G. Chouraqui, C. Aubert and M. Malacria, A molecular approach to self-assembly of trimethylsilylacetylene derivatives on gold, *Chem. – Eur. J.*, 2003, **9**, 2574–2581.

43 S. Watcharinyanon, D. Nilsson, E. Moons, A. Shaporenko, M. Zharnikov, B. Albinsson, J. Mårtensson and L. S. O. Johansson, A spectroscopic study of self-assembled monolayer of porphyrin-functionalized oligo(phenyleneethynylene)s on gold: the influence of the anchor moiety, *Phys. Chem. Chem. Phys.*, 2008, **10**, 5264–5275.

44 G. Jayamurugan, V. Gowri, D. Hernández, S. Martín, A. González-Orive, C. Dengiz, O. Dumele, F. Pérez-Murano, J.-P. Gisselbrecht, C. Boudon, W. B. Schweizer, B. Breiten, A. D. Finke, G. Jeschke, B. Bernet, L. Ruhlmmann, P. Cea

 This journal is © The Royal Society of Chemistry 2019

Open Access Article. Published on 07 August 2019. Downloaded on 3/28/2024 8:15:32 PM.
This article is licensed under a Creative Commons Attribution 3.0 Unported Licence.

and F. Diederich, Design and synthesis of Aviram–Ratner-type dyads and rectification studies in Langmuir–Blodgett (LB) films, *Chem. – Eur. J.*, 2016, **22**, 10539–10547.

45 Z. Wei, X. Wang, A. Borges, M. Santella, T. Li, J. K. Sørensen, M. Vanin, W. Hu, Y. Liu, J. Ulstrup, G. C. Solomon, Q. Chi, T. Bjørnholm, K. Nørgaard and B. W. Laursen, Triazatriangulene as Binding Group for Molecular Electronics, *Langmuir*, 2014, **30**, 14868–14876.

46 C. Atienza, N. Martin, M. Wielopolski, N. Haworth, T. Clark and D. M. Guldi, Tuning electron transfer through p-penyleneethynylene molecular wires, *Chem. Commun.*, 2006, 3202–3204.

47 S. Martin, W. Haiss, S. Higgins, P. Cea, M. C. Lopez and R. J. Nichols, A comprehensive study of the single molecule conductance of alpha,omega-dicarboxylic acid-terminated Alkanes, *J. Phys. Chem. C*, 2008, **112**, 3941–3948.

48 R. M. Metzger, Unimolecular electronics and rectifiers, *Synth. Met.*, 2009, **159**, 2277–2281.

49 L. M. Ballesteros, S. Martín, J. Cortés, S. Marqués-González, S. J. Higgins, R. J. Nichols, P. J. Low and P. Cea, Controlling the structural and electrical properties of diacid oligo(phenylene ethynylene) Langmuir-Blodgett films, *Chem. – Eur. J.*, 2013, **19**, 5352–5363.

50 A. Villares, D. P. Lydon, L. Porres, A. Beeby, P. J. Low, P. Cea and F. M. Royo, Preparation of ordered films containing a phenylene ethynylene oligomer by the Langmuir-Blodgett technique, *J. Phys. Chem. B*, 2007, **111**, 7201–7209.

51 Y. Xing, T. H. Park, R. Venkatramani, S. Keinan, D. N. Beratan, M. J. Therien and E. Borguet, Optimizing Single-Molecule Conductivity of Conjugated Organic Oligomers with Carbodithioate Linkers, *J. Am. Chem. Soc.*, 2010, **132**, 7946–7956.

52 J. C. Li, J. Z. Wu and X. Gong, Conductance switching and photovoltaic effect of Ru(II) complex molecular junctions: role of complex properties and the metal/molecule interface, *J. Phys. Chem. Lett.*, 2014, **5**, 1017–1021.

53 D. Gao, F. Scholz, H.-G. Nothofer, W. E. Ford, U. Scherf, J. M. Wessels, A. Yasuda and F. von Wrochem, Fabrication of Asymmetric Molecular Junctions by the Oriented Assembly of Dithiocarbamate Rectifiers, *J. Am. Chem. Soc.*, 2011, **133**, 5921–5930.

54 F. von Wrochem, D. Gao, F. Scholz, H.-G. Nothofer, G. Nelles and J. M. Wessels, Efficient electronic coupling and improved stability with dithiocarbamate-based molecular junctions, *Nat. Nanotechnol.*, 2010, **5**, 618–624.

55 N. Darwish, D.-P. I., P. Da Silva, N. Tao, J. J. Gooding and M. N. Paddon-Row, Observation of Electrochemically Controlled Quantum Interference in a Single Anthraquinone-Based Norbornylogous Bridge Molecule, *Angew. Chem., Int. Ed.*, 2012, **51**, 3203–3206.

56 Q. Ye, H. Wang, B. Yu and F. Zhou, Self-assembly of catecholic ferrocene and electrochemical behavior of its monolayer, *RSC Adv.*, 2015, **5**, 60090–60095.

57 I. L. Herrer, A. K. Ismael, D. C. Milán, A. Vezzoli, S. Martín, A. González-Orive, I. Grace, C. Lambert, J. L. Serrano, R. J. Nichols and P. Cea, Unconventional Single-Molecule Conductance Behavior for a New Heterocyclic Anchoring Group: Pyrazolyl, *J. Phys. Chem. Lett.*, 2018, **9**, 5364–5372.

58 M. Kiguchi, Y. Takahashi, S. Fujii, M. Takase, T. Narita, M. Iyoda, M. Horikawa, Y. Naitoh and H. Nakamura, Additive Electron Pathway and Nonadditive Molecular Conductance by Using a Multipodal Bridging Compound, *J. Phys. Chem. C*, 2014, **118**, 5275–5283.

59 M. Valášek, M. Lindner and M. Mayor, Rigid multipodal platforms for metal surfaces, *Beilstein J. Nanotechnol.*, 2016, **7**, 374–405.

60 M. A. Karimi, S. G. Bahoosh, M. Valášek, M. Bürkle, M. Mayor, F. Pauly and E. Scheer, Identification of the current path for a conductive molecular wire on a tripodal platform, *Nanoscale*, 2016, **8**, 10582–10590.

61 T. Sebechlebska, J. Sebera, V. Kolivoska, M. Lindner, J. Gasior, G. Meszaros, M. Valasek, M. Mayor and M. Hromadova, Investigation of the geometrical arrangement and single molecule charge transport in self-assembled monolayers of molecular towers based on tetraphenylmethane tripod, *Electrochim. Acta*, 2017, **258**, 1191–1200.

62 M. Valasek and M. Mayor, Spatial and Lateral Control of Functionality by Rigid Molecular Platforms, *Chem. – Eur. J.*, 2017, **23**, 13538–13548.

63 V. Kolivoska, J. Sebera, T. Sebechlebska, M. Lindner, J. Gasior, G. Meszaros, M. Mayor, M. Valasek and M. Hromadova, Probabilistic mapping of single molecule junction configurations as a tool to achieve the desired geometry of asymmetric tripodal molecules, *Chem. Commun.*, 2019, **55**, 3351–3354.

64 S. Gyepi-Garbrah and R. Šilerová, The first direct comparison of self-assembly and Langmuir-Blodgett deposition techniques: Two routes to highly organized monolayers, *Phys. Chem. Chem. Phys.*, 2002, **4**, 3436–3442.

65 G. Pera, A. Villares, M. C. Lopez, P. Cea, D. P. Lydon and P. J. Low, Preparation and characterization of Langmuir and Langmuir-Blodgett films from a nitrile-terminated tolan, *Chem. Mater.*, 2007, **19**, 857–864.

66 A. Villares, G. Pera, S. Martín, R. J. Nichols, D. P. Lydon, L. Applegarth, A. Beeby, P. J. Low and P. Cea, Fabrication, Characterization, and Electrical Properties of Langmuir–Blodgett Films of an Acid Terminated Phenylene–Ethynylene Oligomer, *Chem. Mater.*, 2010, **22**, 2041–2049.

67 L. M. Ballesteros, S. Martin, G. Pera, P. A. Schauer, N. J. Kay, M. Carmen Lopez, P. J. Low, R. J. Nichols and P. Cea, Directionally Oriented LB Films of an OPE Derivative: Assembly, Characterization, and Electrical Properties, *Langmuir*, 2011, **27**, 3600–3610.

68 B. L. M. Hendriksen, F. Martin, Y. Qi, C. Mauldin, N. Vukmirovic, J. Ren, H. Wormeester, A. J. Katan, V. Altoe, S. Aloni, J. M. J. Fréchet, L.-W. Wang and M. Salmeron, Electrical Transport Properties of Oligothiophene-Based Molecular Films Studied by Current Sensing Atomic Force Microscopy, *Nano Lett.*, 2011, **11**, 4107–4112.

69 L. M. Ballesteros, S. Martín, C. Momblona, S. Marqués-González, M. C. López, R. J. Nichols, P. J. Low and P. Cea, Acetylene used as a new linker for molecular junctions in

Open Access Article. Published on 07 August 2019. Downloaded on 3/28/2024 8:15:32 PM.
This article is licensed under a Creative Commons Attribution 3.0 Unported Licence.

phenylene–ethynylene oligomer Langmuir–Blodgett films, *J. Phys. Chem. C*, 2012, **116**, 9142–9150.

70 G. Pera, S. Martin, L. M. Ballesteros, A. J. Hope, P. J. Low, R. J. Nichols and P. Cea, Metal-Molecule-Metal Junctions in Langmuir-Blodgett Films Using a New Linker: Trimethylsilane, *Chem. – Eur. J.*, 2010, **16**, 13398–13405.

71 J. M. Soler, E. Artacho, J. D. Gale, A. Garcia, J. Junquera, P. Ordejon and D. Sanchez-Portal, The SIESTA Method for Ab Initio Order-N Materials Simulation, *J. Phys.: Condens. Matter*, 2002, **14**, 2745–2779.

72 J. Ferrer, C. J. Lambert, V. García-Suárez, D. Z. Manrique, D. Cisontai, L. Oroszlany, R. Rodríguez-Ferradas, I. Grace, S. W. D. Bailey, K. Gillemot, S. Hatef and L. A. Algharagholy, GOLLUM: A nex-Generation Simulation Tool for Electron, Thermal and Spin Transport, *New J. Chem.*, 2014, **16**, 093029.

73 A. K. Ismael, K. Wang, A. Vezzoli, M. K. Al-Khaykanee, H. E. Gallagher, I. M. Grace, C. J. Lambert, B. Su, R. J. Nichols and S. J. Higgins, Side-Group-Mediated Mechanical Conductance Switching in Molecular Junctions, *Angew. Chem., Int. Ed.*, 2017, **56**, 15378–15382.

74 C. Sabater, C. Untiedt, J. J. Palacios and M. J. Caturla, Mechanical Annealing of Metallic Electrodes at the Atomic Scale, *Phys. Rev. Lett.*, 2012, **108**, 205502.

75 M. A. Fernández, C. Sabater, W. Dednam, J. J. Palacios, M. R. Calvo, C. Untiedt and M. J. Caturla, Dynamic Bonding of Metallic Nanocontacts: Insights from Experiments and Atomistic Simulations, *Phys. Rev. B*, 2016, **93**, 085437.

76 L. M. Ballesteros, S. Martin, S. Marqués-González, M. C. López, S. Higgins, R. J. Nichols, P. J. Low and P. Cea, Single gold atom containing oligo(phenylene)ethynylene: assembly into LB films and electrical characterization, *J. Phys. Chem. C*, 2015, **119**, 784–773.

77 S. Y. Quek, M. Kamenetska, M. L. Stigerwald, H. J. Choi, S. G. Louie, M. S. Hybertsen, J. B. Neaton and L. Venkataraman, Mechanically controlled binary conductance switching of a single-molecule junction, *Nat. Nanotechnol.*, 2009, **4**, 230–234.

78 S. Y. Quek, L. Venkataraman, H. J. Choi, S. G. Louie, M. S. Hybertsen and J. B. Neaton, Amine-gold linked single-molecule circuits: experiment and theory, *Nano Lett.*, 2007, **7**, 3477–3482.

79 G. Pera, S. Martin, L. M. Ballesteros, A. J. Hope, P. J. Low, R. J. Nichols and P. Cea, Metal-Molecule-Metal Junctions in Langmuir-Blodgett Films Using a New Linker: Trimethylsilane, *Chem. – Eur. J.*, 2010, **16**, 13398–13405.

80 L. M. Ballesteros, S. Martin, J. Cortes, S. Marques-Gonzalez, S. J. Higgins, R. J. Nichols, P. J. Low and P. Cea, Controlling the Structural and Electrical Properties of Diacid Oligo (Phenylene Ethynylene) Langmuir-Blodgett Films, *Chem. – Eur. J.*, 2013, **19**, 5352–5363.

81 Q. Lu, K. Liu, H. Zhang, Z. Du, X. Wang and F. Wang, From tunneling to hopping: a comprehensive investigation of charge transport mechanism in molecular junctions based on oligo(p-phenylene ethynylene)s, *ACS Nano*, 2009, **3**, 3861–3868.

This journal is © The Royal Society of Chemistry 2019